Author Manuscript

Author Manuscript

Author Manuscript

Author Manuscript

HHS Public Access

Author manuscript

J Heart Valve Dis. Author manuscript; available in PMC 2019 August 07.

Published in final edited form as:

J Heart Valve Dis. 2014 November ; 23(6): 713–720.

A Model of Ischemic Mitral Regurgitation in Pigs with Three-Dimensional Echocardiographic Assessment

Masahito Minakawa[1], **J. Daniel Robb**[1], **Masato Morita**[1], **Kevin J. Koomalsingh**[1], **Mathieu Vergnat**[1], **Matthew J. Gillespie**[2], **Joseph H. Gorman III**[1], **Robert C. Gorman**[1]

[1]Gorman Cardiovascular Research Group, Perelman School of Medicine, University of Pennsylvania, Philadelphia, Pennsylvania, USA

[2]Division of Cardiology, The Children's Hospital of Philadelphia, Philadelphia, Pennsylvania, USA

Abstract

Background and aim of the study: Ischemic mitral regurgitation (IMR), the incidence of which is increasing, results from annular and subvalvular remodeling after myocardial infarction (MI). Although a sheep model of IMR has been used extensively over the past two decades, the ventricular, coronary and leaflet anatomy in sheep is significantly different from that in humans. In contrast, pigs are more similar to humans with regard to these parameters, and therefore may serve as a better animal to test emerging new technologies designed to treat IMR.

Methods: Twenty-nine pigs (body weight 30–35 kg) underwent left thoracotomy and ligation of the mid main circumflex and distal right posterior descending coronary arteries to create a posterolateral MI. Of these pigs, 18 were used for acute data acquisition, while 11 surviving animals in the chronic group were assessed at eight weeks after MI. Real-time three-dimensional echocardiography was performed at baseline, and at 30 min and eight weeks after MI, to assess geometric changes in the mitral annulus, mitral leaflets and left ventricle.

Results: Compared to baseline, the MR grade was increased significantly at eight weeks (0.7 ± 0.5 versus 2.0 ± 1.2), together with a significant decrease in left ventricular ejection fraction (40.3 ± 6.6% versus 25.8 ± 7.7%). Significant increases were also noted at eight weeks in the commissural width (30.1 ± 3.2 mm versus 35.1 ± 2.9 mm) and septolateral diameter (25.0 ± 2.0 mm versus 33.8 ± 5.9 mm), with a resultant increase in mitral annular area (596 ± 85 versus 931 ± 181 mm^3) and a decrease in the annular height to commissural width ratio (15.7 ± 2.6% versus 13.7 ± 1.9%). The mitral valve tenting volume was also increased significantly (1577 ± 645 versus 2440 ± 755 mm^3). The distance between the papillary muscle tips at baseline and at eight weeks was increased significantly (23.9 ± 2.5 versus 30.9 ± 5.2 mm), as was the distance between the posterior papillary muscle tip and the posterior commissure (20.9 ± 2.7 versus 24.1 ± 2.8 mm).

Conclusion: The surgical model described here reliably replicates the changes seen in humans with IMR. Hence, this model can be used for further studies of the pathophysiology of IMR, and of any novel interventions in this challenging clinical area.

Address for correspondence: Robert C. Gorman MD, Gorman Cardiovascular Research Group, Perelman School of Medicine, University of Pennsylvania, Smilow Center for Translational Research, 3400 Civic Center Blvd., Bldg. 421, 11th floor, Room 114, Philadelphia, PA 19104-5156, USA, robert.gorman@uphs.upenn.edu.

Author Manuscript Author Manuscript Author Manuscript Author Manuscript

Ischemic mitral regurgitation (IMR) results from postinfarction remodeling of the left ventricle, whereby valve incompetence results from a combination of annular and subvalvular distortions that produce annular dilatation and leaflet tethering (1). The development of a technique for inducing chronic IMR in sheep was reported 20 years ago (2,3), since which time the present authors and others have used this model extensively to elucidate the pathophysiologic mechanism of IMR. The model has also been used effectively to develop new therapeutic approaches and diagnostic techniques (4–7).

While the ovine model has been extremely useful, it has certain limitations, notably that the sheep coronary anatomy is exclusively left-dominant, which occurs in less than 15% of patients. Pigs are more similar to humans in that they almost always have a right-dominant coronary arterial anatomy. The shape of the sheep left ventricle is also more oblong than in humans, with a pronounced bend near to the apex. Pigs have a three-dimensional (3D) ellipsoidal left ventricular shape that is very similar to that in humans. Finally, sheep leaflets are extremely fragile (especially the posterior leaflet), with the ratio of leaflet tissue area to annular size being much less than that of humans. Pigs and humans have mitral leaflets of similar size, thickness and strength.

Hence, the use of a preclinical model of IMR that has a more human 3D left ventricular shape, and the leaflet properties will likely facilitate the preclinical testing of immerging catheter-based technologies for mitral valve repair, and especially replacement (8). Because of these limitations of the ovine model, the present authors sought to develop a reproducible model of chronic IMR in the pig, and these investigations formed the basis of the present study.

Materials and methods

Animals

A group of 29 Yorkshire swine (body weight 30–35 kg) were used in the present study, and maintained under experimental protocols approved by the University of Pennsylvania’s Institutional Animal Care and Use Committee, in compliance with National Institutes of Health Publication No. 85–23 (revised 1996).

Surgical protocol

Each animal was sedated with intramuscular ketamine (25–30 mg/kg), intravenous glycopyrrolate (0.02 mg/kg) and intramuscular buprenorphine (0.005 mg/kg), and then intubated and mechanically ventilated (Hallowell EMC Model AWS; Pittsfield, Massachusetts, USA) using isoflurane (1.5–2.0%) and room air with oxygen at 0.6 l/min.

The arterial blood pressure was monitored through a 7 Fr sheath inserted into the carotid artery, and an intravenous line was placed in the internal jugular vein via a medial neck incision. The arterial blood pressure and electrocardiogram were monitored throughout the operation. Maximum and minimum dP/dt were measured with a high-fidelity pressure transducer in the left ventricle (SPC-350; Millar Instruments, Inc., Houston, Texas, USA). The central venous pressure (CVP), pulmonary artery pressure (PAP), pulmonary capillary

Author Manuscript Author Manuscript Author Manuscript Author Manuscript

wedge pressure (PCWP) and cardiac output (CO) were measured using a SwanGanz catheter.

A small left thoracotomy was performed via the fifth intercostal space. Following opening of the pericardium, baseline 3D echocardiographic data were acquired to assess the left ventricular and mitral valve 3D anatomy. A posterolateral myocardial infarction (MI) was created by ligating the main circumflex coronary artery just distal of the first obtuse marginal artery, and the right posterior descending artery at a level of 1.5 cm distal from the atrioventricular groove (Fig. 1A). Echocardiographic data were recorded again at 30 min after MI. In order to limit ventricular arrhythmias, amiodarone (100 mg) was administered via a central vein over a 5-min period prior to thoracotomy, followed by continuous infusion at a rate of 2.0–3.0 mg/kg/h for 1 h. Additionally, lidocaine (9–18 mg) was administered by bolus just prior to ligation of the coronary arteries. In case of ventricular fibrillation or tachycardia, the heart was defibrillated (50 J/s) and additional lidocaine administered. Neosynephrine was given in small boluses to maintain a mean arterial pressure of 75–80 mmHg before and immediately after coronary occlusion. Using this pharmacologic approach, ventricular fibrillation occurred in less 10% of animals, and cardioversion was always successful.

Following the 30-min post-MI echocardiographic study, the pigs were allocated to two groups, namely acute and chronic. In the acute group, 14 pigs were euthanized at 3 h after coronary occlusion to allow assessment of the infarct size and location, using an Evans blue dye staining technique (9). In the chronic group, 15 pigs were allowed to recover and returned to the operating room eight weeks after the MI, where they were anesthetized and monitored as described above. Three-dimensional (3D) echocardiographic images and hemodynamic data were recorded both at rest and during increasing hemodynamic stress induced by the administration of dobutamine at 5 or 10 μg/kg/min. After image acquisition and hemodynamic data collection, the animals were euthanized. Four animals in the chronic group died before the eight-week study; hence, 11 pigs were investigated at eight weeks post MI.

Echocardiographic protocol and analysis

Epicardial real-time 3D echocardiography was performed using an iE33 instrument (Philips Medical Systems, Bothell, Washington, USA), equipped with a 2- to 7-MHz probe (xMATRIX array probe X7–2; Philips). Each full-volume dataset was then exported to an Echo-View 5.4 (TomTec Imaging Systems, Munich, Germany) workstation for image analysis. Images were analyzed to assess mitral annular and leaflet 3D geometry as well as left ventricular volumes.

The left ventricular end-diastolic volume (LVEDV), left ventricular end-systolic volume (LVESV) and left ventricular ejection fraction (LVEF) were calculated by tracing endocardial surface lines manually in both end-diastolic and end-systolic frames of one cardiac cycle.

The mitral valve analysis was performed at midsystole, as described previously (10–12). Briefly, the plane of the mitral valve orifice was rotated into a short-axis view, and the

Author Manuscript Author Manuscript Author Manuscript Author Manuscript

geometric center then translated to the intersection of the two corresponding long-axis planes, which corresponded to the intercommissural and septolateral axes of the mitral valve orifice. A rotational template consisting of 18 long-axis cross-sectional planes separated by 10° increments was superimposed on the 3D echocardiogram. The two annular points intersecting each of the 18 long-axis rotational planes were then identified by means of orthogonal visualization of each plane; the two annular points were marked interactively (total of 36 annular points). Measurement planes were marked at fixed, 1-mm intervals along the entire length of the intercommissural axis. In each two-dimensional plane, data points delineating the anterior and posterior leaflets were traced across the atrial surfaces, resulting in a 500-point to 1000-point dataset for each valve. For the coaptation tracing, meticulous care was taken to clearly identify the tip of both anterior and posterior leaflets immediately before coaptation (using previous frames), so that the highest (most atrial) and lowest (most ventricular) margins of the coaptation zone could be defined. These atrial and ventricular edges of the coaptation zone were then marked interactively. Anterior and posterior commissures were defined as annular points at the junction between the anterior and posterior leaflets (middle of commissural region) and interactively identified. The X, Y, and Z coordinates of each data point, assigned to the annulus, anterior leaflet, posterior leaflet or the coaptation surface, respectively, were then exported to Matlab (Mathworks, Inc., Natick, MA, USA), which allowed rendering of mitral annular and leaflet anatomy. The tips of the anterior and posterior papillary muscles were also identified. The center of gravity of the resultant 36-point annular data set was translated to the origin. The least squares plane of the 3D dataset was then calculated and the annular model rotated such that this mitral valve annular plane was aligned with the x-y plane. Mitral annular area (MAA) was defined as the area enclosed by the 2D projection of a given annular data set onto its corresponding least squares plane.

Annular height (AH) was defined as the distance between the middle point of the anterior annulus and a plane that included both anterior and posterior commissures. The intercommissural width (CW) was defined as the distance between the anterior and the posterior commissure. The septolateral diameter was defined as the distance between the middle point of the anterior annulus and the middle point of the posterior annulus. The annular height to commissural height ratio (AH/CW × 100%) was used to quantify global annular non-planarity, as previously reported (13). The mitral annular area was defined as the area enclosed by the two-dimensional projection of an annulus onto its corresponding least-squares plane (14). The tenting area of the mitral valve was defined as the area enclosed by the mitral leaflets and a septolateral line connecting the middle points of the anterior and posterior annuli. The mitral valve tenting index was defined as mitral valve tenting volume/mitral annular area.

The degree of MR was assessed semi-quantitatively with color Doppler by measuring the percentage area of the regurgitation jet in the left atrial area: grade 1 = <20%; grade 2 = 20–40%; grade 3 = 40–60%; and grade 4 = >60% (15).

Author Manuscript Author Manuscript Author Manuscript Author Manuscript

Analysis of infarction area

The heart was excised after euthanization of the animal; the right ventricle and atria were removed and the left ventricular septum was cut longitudinally from the aortic root toward the apex. The left ventricular endocardial photographic image was recorded using a digital camera for the measurement of infarction size, using planimetry software (Image Pro Plus; Media Cybernetics, Inc., USA). In the acute group, the infarct area was visualized using Evans blue, as described previously (Fig. 1B) (9). The infarction area and the entire left ventricular endocardial area were traced manually, and the infarction size was expressed as a percentage of the left ventricular area. The degree to which the infarct involved the mitral annulus was expressed as a percentage of the posterior annulus and the entire mitral annulus that was infarcted. Sections of the myocardium from the infarction were fixed in 5% buffered formalin, paraffin-embedded, sectioned (3–4 μm), and stained with either hematoxylin and eosin or Masson's trichrome stains.

Statistical analysis

All data were expressed as mean ± SD. Comparisons between values at baseline, and at 30 min and eight weeks after infarction (at rest, dobutamine 5 μg/kg/min and dobutamine 10 μg/kg/min) were performed using a one-way repeated ANOVA, followed by the Bonferroni test. All statistical analyses were performed using SPSS II for Windows (SPSS Inc., Chicago, Illinois, USA).

Results

Hemodynamic data

At 30 minutes after the MI, the systolic blood pressure and CO were significantly decreased relative to baseline, but there was a significant increase in PCWP. At eight weeks after the infarct, the minimum dP/dt, PAP, PCWP and CVP were each significantly increased relative to baseline. During dobutamine stress testing, the maximum dP/dt was increased significantly in dose-dependent manner, accompanied by increases in systolic blood pressure and CO (Table I).

Infarct area

An image of the endocardial surface of the left ventricle in a chronic animal at eight weeks after MI is shown in Figure 2A. Considering all animals (both acute and chronic groups), the infarct area was 25.4 ± 5.5% of the left ventricle (acute group 27.9 ± 5.9%; chronic group 24.0 ± 4.9%; $p = 0.3$). The infarct always included the entire posterior papillary muscle and extended to the posterior mitral annulus, and involved 65 ± 20% of the posterior mitral annulus and 41 ± 12% of the entire mitral annular circumference. Pathologic staining demonstrated transmural infarction in all animals (Fig. 2B).

Mitral regurgitation

There was no MR at baseline or at 30 min after infarction, but by eight weeks the MR grade had increased to 2.0 ± 1.2 (Table II; Fig. 3). The mean MR grade was increased to 2.6 ± 1.2 and 2.6 ± 1.3 after 5 and 10 μg/kg/min dobutamine, respectively.

Author Manuscript Author Manuscript Author Manuscript Author Manuscript

Left ventricular volume data

The LVEDV was increased significantly at eight weeks after MI relative to baseline (from 51.9 ± 8.7 ml to 102.0 ± 24.1 ml), as was the LVESV (from 31.2 ± 6.8 ml to 75.8 ± 20.3 ml); however, the LVEF was significantly decreased (from 40.3 ± 6.6% to 25.8 ± 7.7%). Although the administration of dobutamine led to a significant decrease in left ventricular volume, it had no effect on the LVEF.

Three-dimensional mitral valve morphologic data

At eight weeks after MI, the 3D mitral valve analysis demonstrated significant annular and subvalvular remodeling that resulted in pronounced leaflet tethering. The mitral annular area was increased from 596 ± 85 mm^2 at baseline to 931 ± 181 mm^2 during the same time. The distance between the papillary muscle tips increased from 23.9 mm at baseline to 30.9 mm at eight weeks after MI, but both the leaflet tethering volume and tenting index were increased significantly (from 1577 ± 645 ml to 2440 ± 755 ml, and from 2.6 ± 0.8 mm to 3.4 mm, respectively) as a result of annular and subvalvular remodeling. Details of these data are presented in Table III, while the average valve morphology as remodeling progressed and IMR developed is depicted in Figure 4.

Discussion

The aim of the present study was to develop a reproducible model of moderate chronic IMR in pigs by ligating the circumflex coronary artery below the takeoff of the first large circumflex marginal branch, and the posterior descending artery 1.5 cm from the atrioventricular groove. The infarct involved the posterolateral left ventricular wall, the posterior papillary muscle and the posterolateral portion of the mitral annulus, and resulted in moderate IMR by eight weeks after MI.

The size and location of the infarct described was similar to that previously reported in a sheep model, as was the degree of left ventricular remodeling, the annular dilatation, and subvalvular remodeling (2,3). The use of state-of-the art 3D echocardiography and custom image analysis software allowed the effective quantification of valvular and subvalvular remodeling, obviating the need for the sonomicrometry array localization that was used when developing the sheep model (5,16).

Trans-catheter embolization techniques have been described that produce IMR in pigs; however, although these approaches do not require thoracotomy they tend to cause infarcts of widely varying size. A surgical approach through a small thoracotomy would allow for a precise identification of the coronary anatomy and a visual assessment of infarct size, which yields a highly reproducible infarct and, therefore, a consistent remodeling stimulus. In this and previous studies in sheep, an infarct size of between 20–25% of the left ventricular mass has been necessary to yield (reproducibly) a moderate IMR within an eight-week period (2,3).

The use of pigs offers certain benefits over sheep for IMR studies. First, the coronary anatomy of the pig is more similar to that of the human heart. In sheep, the right coronary artery is always poorly developed and never supplies the left ventricle, whereas in pigs - as

Author Manuscript Author Manuscript Author Manuscript Author Manuscript

in humans - it is very commonly a dominant artery with a substantial contribution to the blood supply of the posterolateral left ventricular wall. Second, the shape of the sheep left ventricle is more oblong than in humans, with a pronounced bend near the apex. In fact, pigs have a 3D ellipsoidal left ventricular shape that is very similar to that in humans. Third, the mitral valve leaflets of pigs are more robust and human-like than those of the ovine heart. Fourth, reagents for molecular-biological and genetic analysis are more widely available for pigs than for sheep. It is believed that the human-like characteristics of pig mitral leaflet tissue and left ventricular shape will become important as new catheter-based mitral valve repair and replacement devices are developed, and the need for a clinically relevant large animal model of IMR becomes increasingly important (8).

References

1. Gorman RC, Gorman JH III, Edmunds LH Jr. Ischemic Mitral Regurgitation, in: Cohn LH and Edmunds LH Jr. (ed.), Cardiac Surgery in the Adult. McGraw-Hill, New York, 2003:751–769
2. Llaneras MR, Nance ML, Streicher JT, et al. Pathogenesis of ischemic mitral insufficiency. J Thorac Cardiovasc Surg 1993;105:439–442 [PubMed: 8445923]
3. Llaneras MR, Nance ML, Streicher JT, et al. Large animal model of ischemic mitral regurgitation. Ann Thorac Surg 1994;57:432–439 [PubMed: 8311608]
4. Gorman JH III, Gorman RC, Plappert T, et al. Infarct size and location determine development of mitral regurgitation in the sheep model. J Thorac Cardiovasc Surg 1998;115:615–622 [PubMed: 9535449]
5. Gorman RC, McCaughan JS, Ratcliffe MB, et al. Pathogenesis of acute ischemic mitral regurgitation in three dimensions. J Thorac Cardiovasc Surg 1995;109:684–693 [PubMed: 7715215]
6. Gorman JH III, Gorman RC, Jackson BM, et al. Distortions of the mitral valve in acute ischemic mitral regurgitation. Ann Thorac Surg 1997;64:1026–1031 [PubMed: 9354521]
7. Gorman JH III, Jackson BM, Enomoto Y, Gorman RC. The effect of regional ischemia on mitral valve annular saddle shape. Ann Thorac Surg 2004;77:544–548 [PubMed: 14759435]
8. Gillespie MJ, Minakawa M, Morita M, et al. Sutureless mitral valve replacement: Initial steps toward a percutaneous procedure. Ann Thorac Surg 2013;96:670–674 [PubMed: 23910107]
9. Leshnower BG, Sakamoto H, Hamamoto H, Zeeshan A, Gorman JH III, Gorman RC. The Progression of Myocardial Injury during Coronary Occlusion in the Collateral Deficient Heart: A Non- Wavefront Phenomenon. Am J Physiol Heart Circ Physiol 2007;293:H1799–H1804 [PubMed: 17644569]
10. Ryan LP, Jackson BM, Enomoto Y, et al. Description of regional mitral annular nonplanarity in healthy human subjects: A novel methodology. J Thorac Cardiovasc Surg 2007;134:644–648 [PubMed: 17723812]
11. Ryan LP, Jackson BM, Eperjesi TJ, et al. A methodology for assessing human mitral leaflet curvature using real-time 3-dimensional echocardiography. J Thorac Cardiovasc Surg 2008;136:726–734 [PubMed: 18805278]
12. Vergnat M, Jackson BM, Cheung AT, et al. Saddle- shape annuloplasty increases mitral leaflet coaptation after repair for flail posterior leaflet. Ann Thorac Surg 2011;92:797–804 [PubMed: 21803330]
13. Salgo IS, Gorman JH III, Gorman RC, et al. Effect of annular shape on leaflet curvature in reducing mitral leaflet stress. Circulation 2002;106:711–717 [PubMed: 12163432]
14. Ryan LP, Jackson BM, Parish LM, et al. Regional and global patterns of annular remodeling in ischemic mitral regurgitation. Ann Thorac Surg 2007;84:553–559 [PubMed: 17643634]
15. Miyatake K, Izumi S, Okamoto M, et al. Semiquantitative grading of severity of mitral regurgitation by real-time two-dimensional Doppler flow imaging technique. J Am Coll Cardiol 1986;7:82–88 [PubMed: 3941221]

Author Manuscript Author Manuscript Author Manuscript Author Manuscript

16. Gorman JH III, Gupta KB, Streicher JT, et al. Dynamic three-dimensional imaging of the mitral valve and left ventricle by rapid sonomicrometry array localization. J Thorac Cardiovasc Surg 1996;112:712–726 [PubMed: 8800160]

Author Manuscript Author Manuscript Author Manuscript Author Manuscript

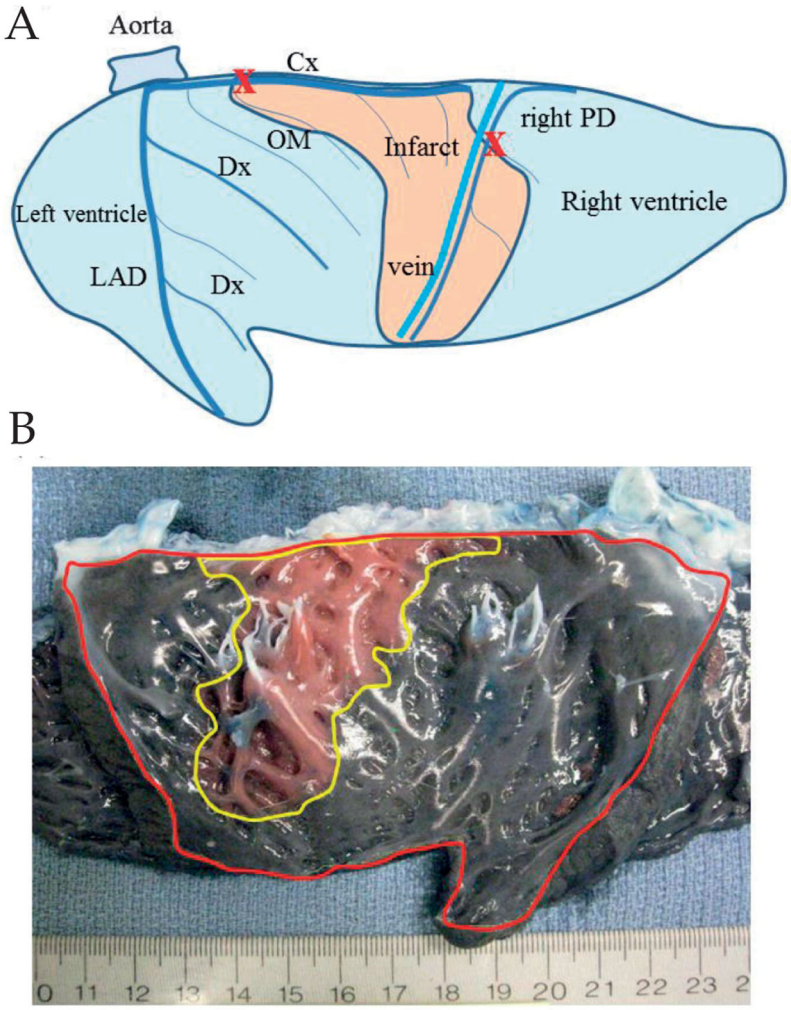

Figure 1:

A) Schematic epicardial view of the left and right ventricle after sectioning through the ventricular septum. A posterolateral myocardial infarction (flesh-colored area) was created by ligating both the main circumflex coronary artery (Cx) just distal of the first obtuse marginal artery (OM) (marked X) and the right posterior descending artery (right PD) at the level of 1.5 cm distal from the atrioventricular groove (marked X). Dx: Diagonal branch;LAD: Left anterior descending artery. B) Photographic endocardial view of the left and right ventricle after sectioning through the ventricular septum (left ventricle outlined in red) in an acute group animal after creating a myocardial infarction. Infarct area (outlined in yellow) is clearly delineated by the injection of Evans blue dye.

Author Manuscript Author Manuscript Author Manuscript Author Manuscript

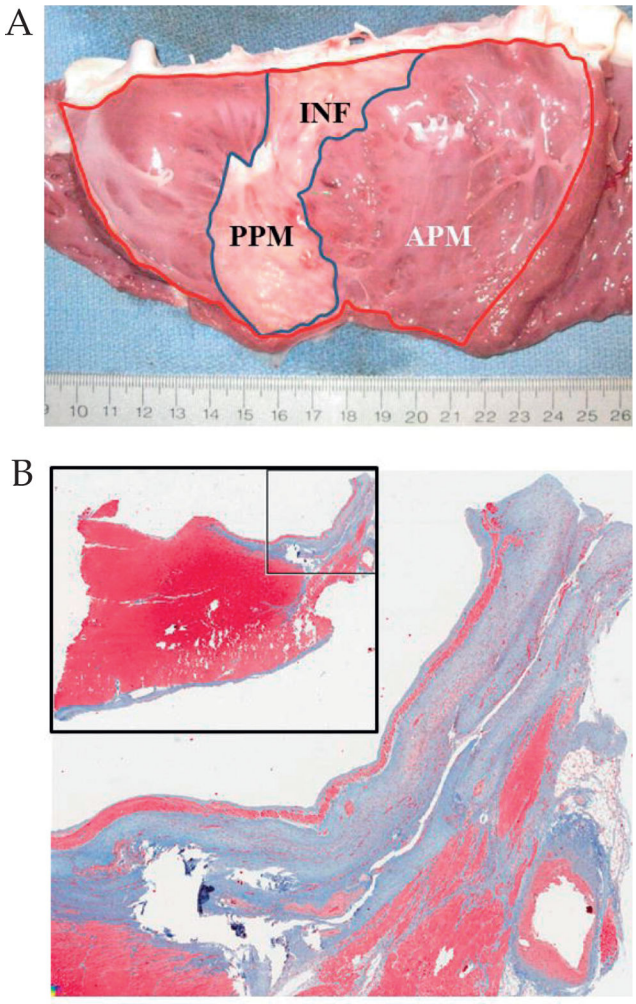

Figure 2:

A) Gross anatomic view of the endocardial side of the opened left ventricle, demonstrating the location of the myocardial infarction, which involves the entire posterior papillary muscle and extends up to the mitral annulus. Infarct size was determined by the ratio of the infarct area (INF; blue line) and the area of the entire left ventricle (red line). B) Masson's trichrome staining demonstrating the transmural nature of the infarct. APM: Anterior papillary muscle; PPM: Posterior papillary muscle.

Author Manuscript Author Manuscript Author Manuscript Author Manuscript

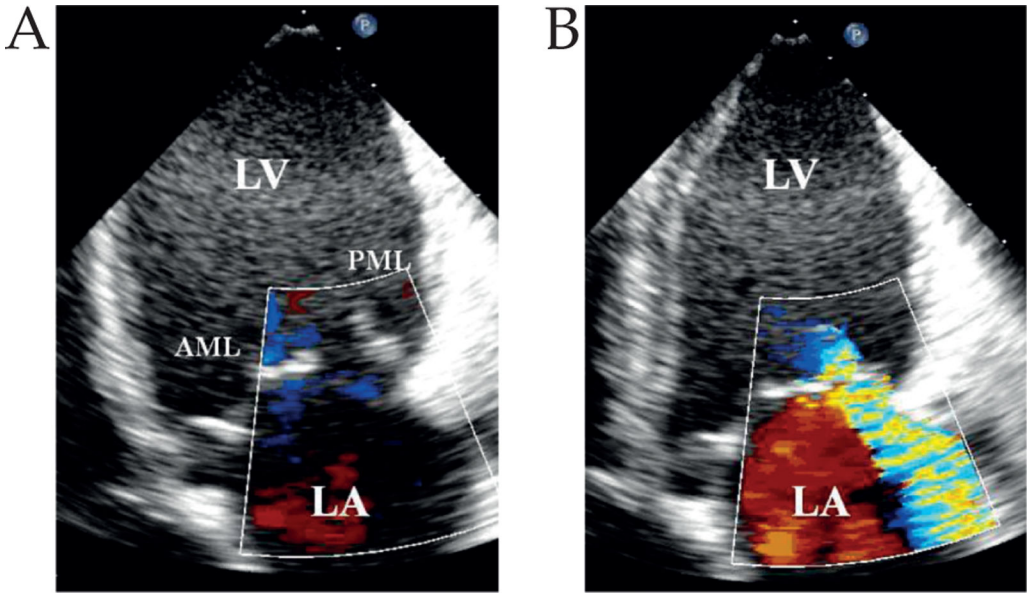

Figure 3:

A) Echocardiography at eight weeks after infarction, demonstrating dilatation of the lateral wall of the left ventricle and tethering of the posterior mitral leaflet. B) Representative Doppler color flow image demonstrating moderate MR jet directed toward posterior wall of the left atrium (LA). LV: Left ventricle; AML: Anterior mitral leaflet; PML: Posterior mitral leaflet

Author Manuscript Author Manuscript Author Manuscript Author Manuscript

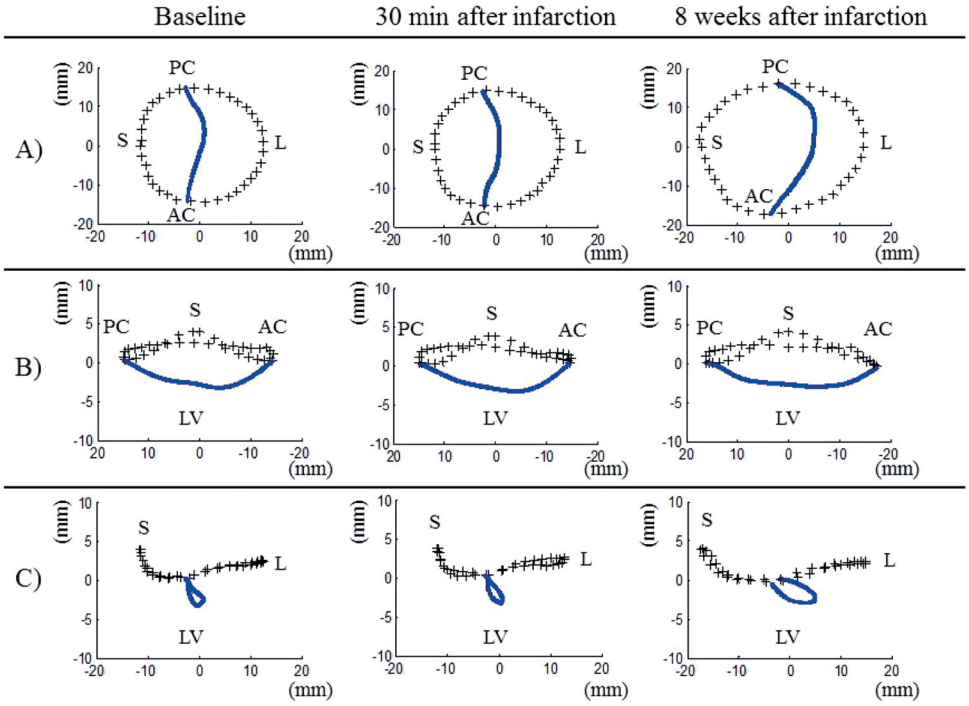

Figure 4:

Average three-dimensional plots of mitral valve annual (+++) and leaflet coaptation (blue line) that resulted from the mitral valve segmentation algorithm described in the text. A) Valve viewed from above. B) Septolateral view (looking over the saddle horn towards the posterior annulus). C) Intercommissural view. Plots were created at the time of baseline, at 30 min after infarction, and at eight weeks after infarction. Note the progressive annular dilatation, annular flattening and posterior displacement of the coaptation line over time. AC: Anterolateral commissure; PC: Posterolateral commissure; S: Septum (middle of anterior area); L: Lateral (middle of posterior area); LV: Left ventricle.

Author Manuscript Author Manuscript Author Manuscript Author Manuscript

Table I:

Hemodynamic data.

Hemodynamic parameter	Baseline	30 min post MI	Eight weeks after MI		
			Resting 5 μg/kg/min	Dobutamine 10 μg/kg/min	Dobutamine
Systolic ABP (mmHg)	89.0 ± 9.6	81.1 ± 9.3[a]	88.1 ± 9.9	97.8 ± 12.9[b]	99.6 ± 14.9[b]
Systolic PAP (mmHg)	29.2 ± 4.6	31.2 ± 7.8	35.1 ± 2.3[a]	35.8 ± 3.0	37.2 ± 2.0[b]
Maximum dP/dt (mmHg/s)	909 ± 244	988 ± 464	840 ± 158[d]	1529 ± 377[a,b,c]	2284 ± 436[a,b,c,d]
Minimum dP/dt (mmHg/s)	−1151 ± 257	−986 ± 473	−963 ± 159[a]	−1251 ± 221	−1646 ± 495[a,b,c]
PCWP (mmHg)	13.7 ± 3.3	17.1 ± 6.7[a]	20.3 ± 3.8[a]	20.3 ± 3.5[a]	18.3 ± 3.7[a]
CVP (mmHg)	11.4 ± 4.4	11.6 ± 3.9	17.3 ± 3.5[a,b]	16.7 ± 2.6[a,b]	14.0 ± 3.2
Cardiac output (1/min)	3.5 ± 1.0	3.1 ± 0.6	4.5 ± 1.6[b]	7.1 ± 2.4[a,b,c]	6.7 ± 1.9[a,b,c]

All values are mean ± SD.

ABP: Arterial blood pressure; CVP: Central venous pressure; MI: Myocardial infarction; PAP: Pulmonary artery pressure; PCWP: Pulmonary capillary wedge pressure.

[a] p <0.05 versus baseline;

[b] p <0.05 versus 30 min after MI;

[c] p <0.05 versus resting condition;

[d] p <0.05 versus dobutamine 5 μg/kg/min.

J Heart Valve Dis. Author manuscript; available in PMC 2019 August 07.

Author Manuscript Author Manuscript Author Manuscript Author Manuscript

Table II:

Left ventricular volume and mitral regurgitation (MR) data.

Measurement	Baseline	30 min post MI	Eight weeks after MI		
			Resting	Dobutamine 5 μg/kg/min	Dobutamine 10 μg/kg/min
MR grade	0.7 ± 0.5	0.9 ± 0.7	2.0 ± 1.2[a,b]	2.6 ± 1.2[a,b]	2.6 ± 1.3[a,b]
LVEF (%)	40.3 ± 6.6	31.4 ± 5.8[a]	25.8 ± 7.7[a]	29.8 ± 7.5[a]	32.6 ± 10.7[a]
LVEDV (ml)	51.9 ± 8.7	57.9 ± 8.5	102.0 ± 24.1[a,b]	84.4 ± 24.0[a,b,c]	70.6 ± 19.1[a,b,c,d]
LVESV (ml)	31.2 ±6.8	39.8 ± 7.3[a]	75.8 ± 20.3[a,b]	59.6 ± 20.8[a,b,c]	47.7 ± 16.1[a,c]

All values are mean ± SD.

LVEDV: Left ventricular end-diastolic volume; LVEF: Left ventricular ejection fraction; LVESV: Left ventricular end-systolic volume; MI: Myocardial infarction.

[a] p <0.05 versus baseline;

[b] p <0.05 versus 30 min after MI;

[c] p <0.05 versus resting condition,

[d] p <0.05 versus dobutamine 5 μg/kg/min.

Author Manuscript Author Manuscript Author Manuscript Author Manuscript

Table III:

Systolic mitral valve morphologic data.

Dimension	Baseline	30 min after MI	Eight weeks after MI
Mitral annular area (mm^2)	596 ± 85	621 ± 138	931 ± 181[a,b]
Tenting volume (ml)	1577 ± 645	1878 ± 913	2440 ± 755[a,b]
Tenting index (mm)	2.6 ± 0.8	2.9 ± 1.0	3.4 ± 0.9[a,b]
Annular height (mm)	4.6 ± 0.5	4.7 ± 1.5	4.7 ± 0.5
Intercommissural width (mm)	30.1 ± 3.2	29.4 ± 3.1	35.1 ± 2.9[a,b]
Annular height:intercommissural width ratio (%)	15.7 ± 2.6	16.7 ± 4.4	13.7 ± 1.9
Septolateral diameter (mm)	25.0 ± 2.0	25.4 ± 3.5	33.8 ± 5.9[a,b]
ALPM to center (mm)	21.4 ± 3.2	20.8 ± 1.8	23.7 ± 1.8[a,b]
ALPM to ALC (mm)	20.7 ± 3.1	19.7 ± 2.0	22.8 ± 3.0[b]
ALPM to PMC (mm)	32.6 ± 3.8	31.6 ± 2.6	35.9 ± 3.4[a,b]
PMPM to center (mm)	22.2 ± 2.7	21.8 ± 2.1	29.0 ± 3.6[a,b]
PMPM to ALC (mm)	34.4 ± 3.9	34.3 ± 3.3	43.7 ± 4.5[a,b]
PMPM to PMC (mm)	20.9 ± 2.7	20.2 ± 1.2	24.1 ± 2.8[a,b]
ALPM to PMPM (mm)	23.9 ± 2.5	25.0 ± 3.4	30.9 ± 5.2[a,b]

All values are mean ± SD.

ALC: Anterolateral commissure; ALPM: Anterolateral papillary muscle; MI: Myocardial infarction; PMC: Posteromedial commissure; PMPM: Posteromedial papillary muscle.

[a] p <0.05 versus baseline;

[b] p <0.05 versus 30 min after MI.